Catastrophic Collision Between Obesity and COVID-19 Have Evoked the Computational Chemistry for Research in Silico Design of New CaMKKII Inhibitors Against Obesity by Using 3D-QSAR, Molecular Docking, and ADMET

Halima Hajji* [ID] [a], Fatima En-nahli [ID] [a], Ilham Aanouz [ID] [a], Hanane Zaki [ID] [b],Tahar Lakhlifi [ID] [a], Mohammed Aziz Ajana* [ID] [a], and Mohammed Bouachrine [ID] [a,b].

The purpose of the paper is to discuss the various methods and computational approaches, which are used in computer-aided drug design. For this reason, pyrimidine and azaindole derivatives have been used to study the inhibitory activity of CaMKKII. It is an enzyme that enters the brain to greatly reduce food from regulating the production of Ghrelin that is synthesized by the stomach and acts on the hypothalamus. The obtained results from different techniques such as the 3D-QSAR, molecular docking, and ADMET were applied to study series of new CaMKKII inhibitors of 23 molecules based on pyrimidine and azaindole derivatives. The CoMFA and CoMSIA models were used in 19 molecules in the training set that give high values of determination coefficient R^2 0.970 and 0.902 respectively, and significant values of Leave-One-Out cross-validation coefficient Q^2 0.614 and 0.583 respectively. The predictive capacity of this model was examined by external validation though using a test set of four compounds with a predicted determination coefficient test R^2_{ext} of 0.778 and 0.972 successively. The method of alignment adapted with the appropriate parameters gave credible models. The CoMFA and CoMSIA models produce the contour maps which were used to define a 3D-QSAR mode.

Graphical abstract
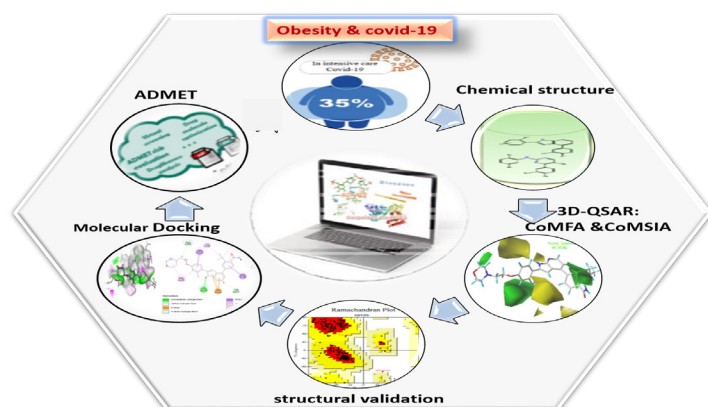
[a] Molecular chemistry and Natural Substances Laboratory, Faculty of Science, University Moulay Ismail, Meknes, Morocco. Corresponding author. [b] Superior School of Technology - Khenifra (EST-Khenifra), University of Sultan My Slimane, PB 170, Khenifra 54000 Morocco. *Corresponding author. E-mail: **a.ajanamohammed@fs.umi.ac.ma**

1. Introduction

The current 2019 coronavirus disease (COVID-19) outbreak has is considered as a rapidly universal progress health crisis that challenges the world and poses public health concerns and overlaps with another well-known pandemic in our society, abundance which is about overweight and obesity [1]. The last one is a chronic inflammatory disease that is increasingly shown to be an increased danger factor for severe COVID-19 infection, leading patients to intensive care units (ICUs) for respiratory assistance with the threat of death (Figure 1) [2–4].

Obesity is not a lifestyle choice, but it is a disease recognized by the World Health Organization WHO, it increases the risk of hospitalization following Covid-19 and expands the risk of dying by nearly 50%, according to a global analysis [5]. It affects lung function in several ways that are related to mechanical and inflammatory aspects, which makes the majority of obese people suffer from respiratory symptoms and progress to respiratory failure. It is a danger factor for diabetes, hypertension, cholesterol ... And faced with Covid-19, we noticed that nearly 1 in 2 patients in intensive care are obese with an enfeeble immune system,

which can make this category unprotected from this serious form of Covid-19 [6-8]. The risk related to obesity could be particularly relevant in the United States as the prevalence of obesity is around 40% [8], 24% in Spain, and 20% in Italy against a prevalence of 6.2% in China [9-10]. According to the WHO, we talk about obesity when the body mass index (BMI) exceeds the threshold of 30 kg/m^2, it is calculated simply by dividing the weight (in kg) by the square of the height (m). The normal BMI is between 18.5 and 25 kg/m^2. The researchers also have informed that a coronavirus vaccine may be unsuccessful on obese people. This conclusion is established on the fact that influenza vaccines such as H_1N_1 do not work well enough in people with a body mass index (BMI) greater than 30 [11-12]. A report from the United States also represented that among Covid-19 patients under the age of 60, those with a BMI of 30-35 kg/m^2 and above 35 kg/m^2 had 1.8 and 3.6 are more likely to be admitted to intensive care. People with a BMI <30 (kg/m^2) [13]. For example, studies in China have shown that the presence of obesity increases the danger of severe Covid-19, almost about three times, resulting in the length of hospital stay [14].
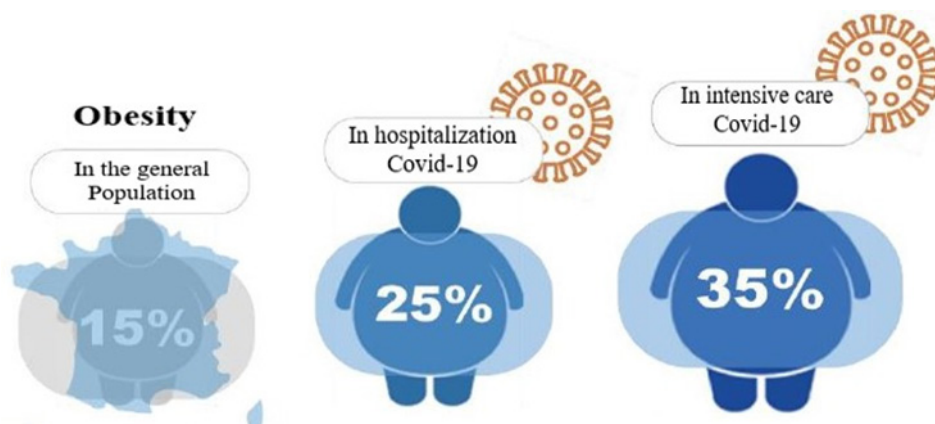

Fig. 1. The importance of obesity in severe forms of COVID-19 infections.

Recent research on obesity suggests that some of the defects responsible for this condition are due to impaired responsiveness of key hypothalamic neurons to several metabolic signals such as leptin, ghrelin, insulin, glucose, and fatty acids [15]. For this reason, pyrimidine and azaindole derivatives have been used to study the inhibitory activity of Ca^{++} / calmodulin-dependent protein kinase II (CaMKKII) which is an enzyme that enters the brain when administered orally [16-17], to control insulin signaling, because the increase of insulin in the blood causes an increase in adiposity in the white adipose tissue, which then stimulates the secretion of leptin (the hormone of satiety) this increase acts on the hypothalamus by causing the inhibition of food intake in the individual [18-19]. Also, CaMKKII greatly reduces the diet by regulating the production of Ghrelin (the hunger hormone) that is produced by the stomach and acts on the hypothalamus (Figure 2) [20-21].

In this research we shed light on series of 23 molecules based on pyrimidine and azaindole derivatives and predict their activity against obesity by using the QSAR study which has crossed a decisive threshold both from a theoretical point of view and practice with the appearance of methods that are based on descriptors of three-dimensional structures such as CoMFA and CoMSIA, this kind of QSAR study is commonly

called 3D-QSAR [22]. To go further in our research, we are continuing this work using more techniques. advanced molecular docking and ADMET [23-24].
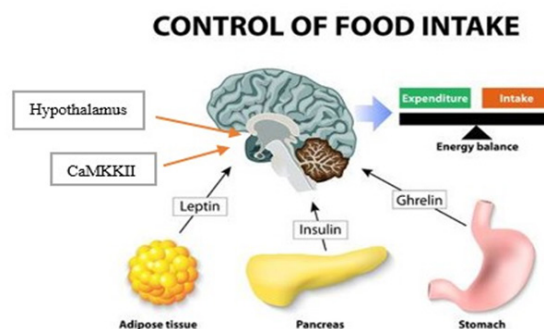

Fig. 2. Ghrelin and leptin - hormones that regulate appetite using CAMKKII inhibitor.

2. Material and Methods

Dataset

In the 3D-QSAR studies, a database of 23 molecules

consisting of pyrimidine and azaindole derivatives (Figures 3 and 4) as CAMKKII inhibitors were taken from published study [25] and divided into two groups; 19 compounds were considered to be a group of training and 4 compounds were sorted out as the whole test, by being focused on a random selection to assess the ability of the resulting model. The structures and biological activities of the training and test sets are shown in Figure 5 and Table 1. These data sets were utilized to structure a model 3D-QSAR and to analyze their physicochemical properties. The biological activities IC$_{50}$ (µM) were previously measured in µM/mL. We transformed them into corresponding pIC$_{50}$ values and have listed them with their corresponding structures (Figure 5 and Table 1) which were used as dependent variables in all subsequently developed PLS models.

Molecular modeling and molecular alignment

The CoMFA and CoMSIA studies are components of the QSAR model of the SYBYL-X2.0 software [26]. To build and optimize the 3D structure. the 23 molecules studied was fully optimized in geometry by using the standard force field of tripos molecular mechanics and the energy gradient convergence criterion (0.01 kcal/mol) [27], the partial atomic charges necessary for the calculation of electrostatic potential are assigned using the training Gasteiger_Huckel [28]. The results obtained by this 3D-QSAR model require aligning the molecules on the common CORE, it is a rather delicate step done by Sybyl utilizing the most active

compound 21 as a model [29]. Figure 6 shows the alignment of the 3D structure of the training set.
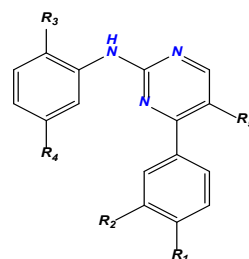

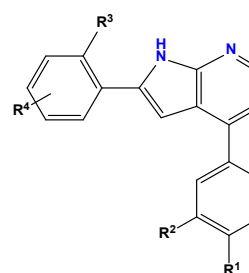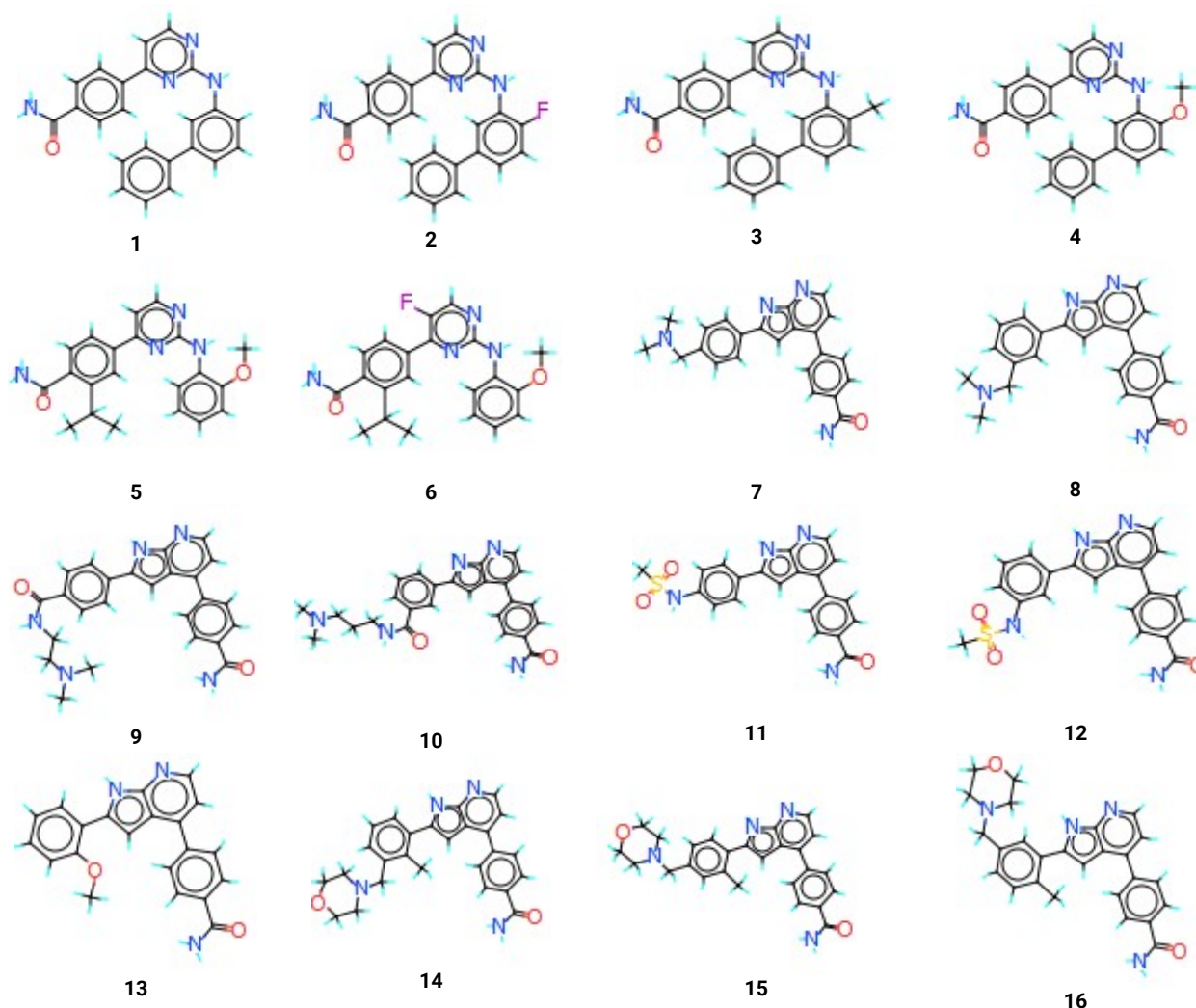**Fig. 3.** The chemical structure of the 2-anilino,4-aryl pyrimidines.

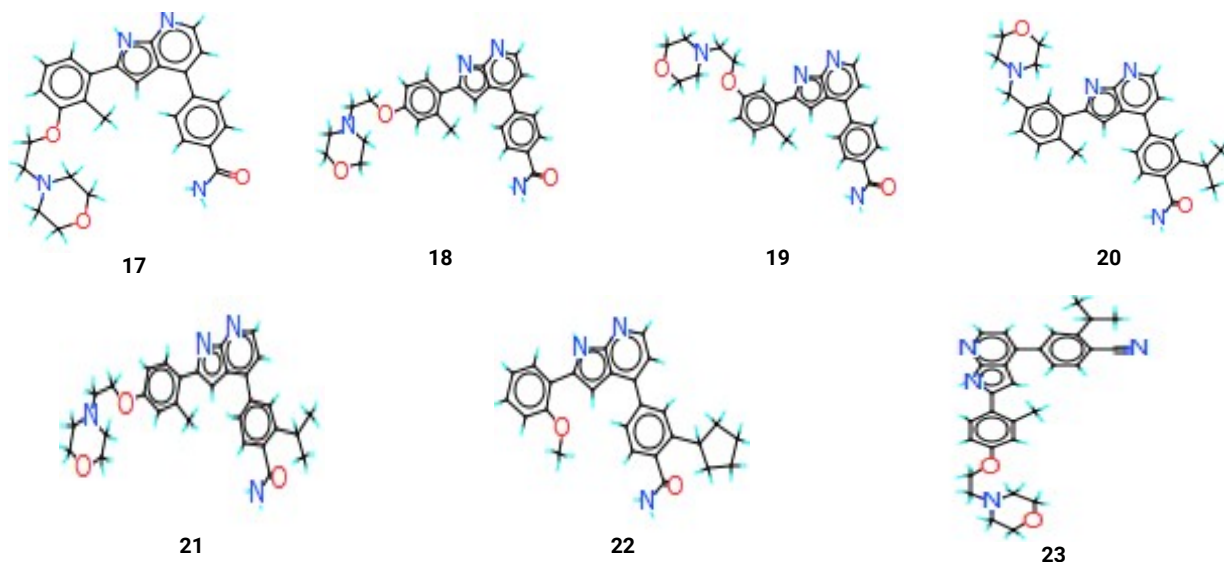**Fig. 4.** The chemical structure of the 2,4-diaryl 7-azaindoles.

Fig. 5. Chemical structures of compounds under study.

Table 1. Experimental activities of the studied compounds.

N	R₁	R₂	R₃	R₄	R₅	pIC₅₀
1	$CONH_2$	H	H	Phenyl	H	8.1
2	$CONH_2$	H	F	Phenyl	H	7.7
3	$CONH_2$	H	CH_3	Phenyl	H	7.5
4	$CONH_2$	H	OCH_3	Phenyl	H	7.9
5	$CONH_2$	Isopropyl	OCH_3	H	H	7.2
6	$CONH_2$	Isopropyl	OCH_3	H	F	7.4
7	$CONH_2$	H	H	P-$CH_2N(CH_3)_2$	-	8.5
8	$CONH_2$	H	H	m-$CH_2N(CH_3)_2$	-	8.4
9	$CONH_2$	H	H	P-$CONH(CH_2)_3N(CH_3)_2$	-	8.8
10	$CONH_2$	H	H	m-$CONH(CH_2)_3N(CH_3)_2$	-	8.6
11	$CONH_2$	H	H	P-$NHSO_2CH_3$	-	8.7
12	$CONH_2$	H	H	m-$NHSO_2CH_3$	-	8,5
13	$CONH_2$	H	OCH_3	H	-	8.5
14	$CONH_2$	H	CH_3	3-CH_2-morpholine	-	8.8
15	$CONH_2$	H	CH_3	4-CH_2-morpholine	-	8.1
16	$CONH_2$	H	CH_3	5-CH_2-morpholine	-	8.8
17	$CONH_2$	H	CH_3	3-$O(CH_2)_2$-morpholine	-	8.7
18	$CONH_2$	H	CH_3	4-$O(CH_2)_2$-morpholine	-	8.8
19	$CONH_2$	H	CH_3	5-$O(CH_2)_2$-morpholine	-	8.7
20	$CONH_2$	isopropyl	CH_3	5-CH_2-morpholine	-	8.8
21	$CONH_2$	isopropyl	CH_3	4-$O(CH_2)_2$-morpholine	-	9.1
22	$CONH_2$	cyclopentyl	OCH_3	H	-	8.7
23	CN	isopropyl	CH_3	4-$O(CH_2)_2$-morpholine	-	8.2

3D QSAR: CoMFA and CoMSIA analyses

CoMFA studies

The CoMFA methods were the first 3D-QSAR approaches developed. The basic idea of CoMFA studies is mainly about the differences in biological activity between molecules are often explained by differences in the shape and strength of the non-covalent interaction fields surrounding the molecules. In other words, the steric and electronic fields would be sufficient to understand the biological properties of a set of compounds and to find a better model on high values of Q^2 and R^2, with a low standard error of estimate (SEE). These interaction fields are performed at every point of intersection of an ordered 2 Å divergence grid, and a cutoff energy value is set by default at 30 kcal/mol [30]. The regression analysis employed is the cross-validation PLS method. The filtering of the column is set at 2.0 kcal/mol [31].

CoMSIA studies

The CoMSIA method is a modified version of CoMFA which uses, in addition to steric and electrostatic interaction fields, a lipophilic interaction field, a "hydrogen bond acceptor" field, and a "hydrogen bond donor" field. the difference between the two methods is also associated with the way they calculate the molecular interaction fields. They generally give comparable results, but the CoMSIA method gives richer and easier to interpret results compared to the CoMFA method.
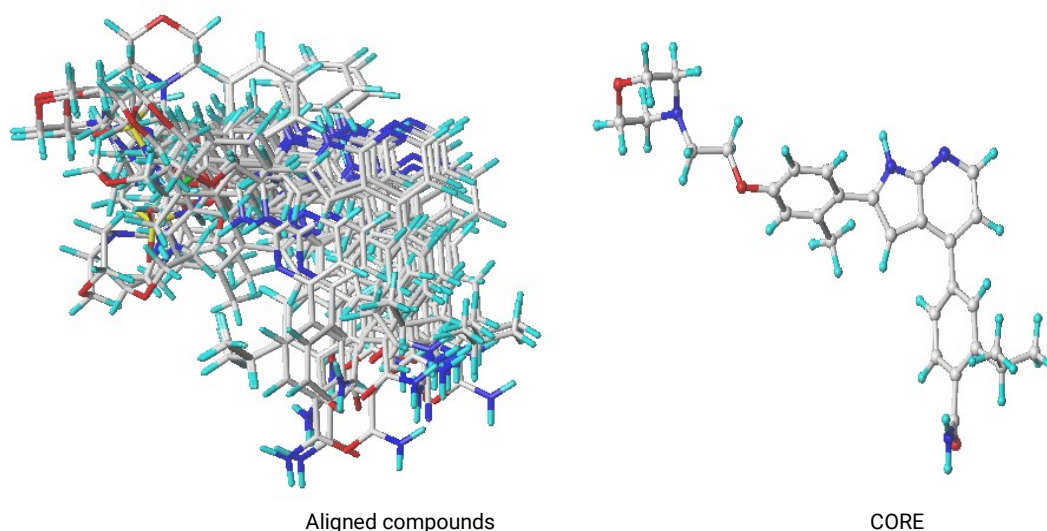
Aligned compounds   CORE

Fig. 6. 3D structure alignment of the training set and the core.

Partial least square (PLS) analysis

The first study was about PLS which was performed for the LOO cross-validation analysis. The characteristics of the best model must have the following criteria: satisfactory values of F, $Q^2 \geq 0.5$, and $R^2 \geq 0.6$ as well as preferences that Nmax the maximum number of components is less than or equal to 1/5 of the number of molecules in the learning game, without forgetting S_{cv} which must have a low value. through this "PLS" technique that we can visualize a model and use it to predict anti-obesity activity [32].

Molecular docking

The use of docking methods in the drug design process began over 30 years ago [33]. This method is considered one of the most important techniques for discovering new small molecule drugs. Their goal is to predict whether or not a molecule can bind to the active site of a protein, based on the prediction of the conformation and orientation of the molecule when it binds to the receptor [34]. To sum up, the docking methods combine the use of a search algorithm, making it possible to generate putative modes of ligand binding in the receptor, or "poses", and a score function used to classify the ligands. different poses according to a predicted score of affinity [35]. Thus, the docking methods, therefore, focus, on the one hand, on identifying the molecules which are true ligands of the receptor among all those studied. Otherwise, on determining the correct poses or the conformations adopted by the ligands when binding to the receptor. In our research, we performed the molecular docking study of the two compounds, compound 21 which is the most active, and compound 5 which is the least active. The docking protocol was performed via the Surflex-dock method by using Sybyl, the results were visualized and analyzed using Pymol [36] and Discovery studio [37] software successively.

Macromolecular preparation

The 3D crystal structure of CaMKKII is downloaded from the Protein Data Bank from the link RCSB (PDB ID = 2ZV2), the studio discovery software was applied to the protein to prepare it and clean it, plus removing the water molecules and adding hydrogen atoms of the receptor to the prepared structure.

Ligand preparation

the most active and least active molecules 21 and 5 respectively that belong to a series of 23 molecules based on pyrimidine and azaindole derivatives were geometrically optimized and energetically minimized using default parameters. These studied compounds were anchored in the protein site.

In silico pharmacokinetics ADMET

After examining the interactions of more active and less active molecules with protein by using molecular docking, then proceeds to the in silico ADMET study which was carried out, the interest them is to examine the capacity of these molecules to become a drug and eliminate weak candidates (Figures 7 and 8).

3. Results and Discussion

CoMFA results

Coming from the results shown in the table, we see that the CoMFA model has a high correlation coefficient R^2 (0.970), cross-correlation coefficient Q^2 (0.614), an F-test value (163, 736), and a low standard error of the estimate S_{cv} (0.098) with three as the optimal number of components. Also, this CoMFA model indicated different steric and electrostatic field contributions of 0.417 and 0.583. The four randomly selected test sets were optimized and aligned in the same way as the training sets. External validation gave a large value of R^2_{ext} (0.778), which indicates that the predictive capacity of the CoMFA model is allowable.

CoMSIA results

CoMSIA descriptors were designed by using SYBYL software, a 3D-QSAR model has been proposed to explain and quantitatively predict the effects of the hydrophobic, electrostatic, steric, donor, and acceptor fields of the substituents on the inhibitory activity of CAMKKII against obesity. Of a series of 23 molecules based on pyrimidine and azaindole derivatives. Many combinations of the five fields "S, E, H, D, A" were examined to design the best CoMSIA model and the results are detailed in Table 2. They indicated that the value of the cross-validated correlation coefficient of the training set Q^2 and the correlation coefficient R^2 are respectively 0.583 and 0.902, The standard error was low

0.172. Therefore, the prediction capacity of the proposed model is confirmed by using external validation, the R2ext value obtained is 0.973. These statistical results indicate the good stability and the powerful predictive capacity of the CoMSIA model presented in Table 2.
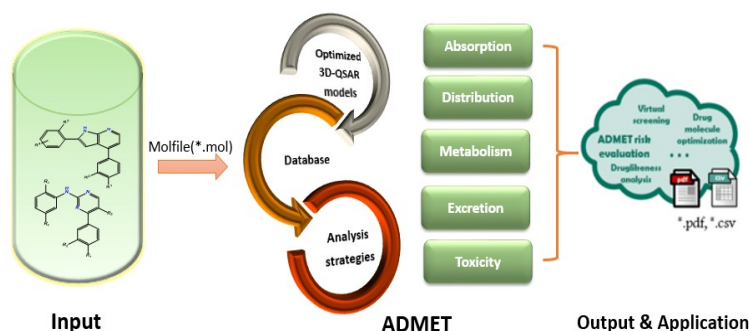

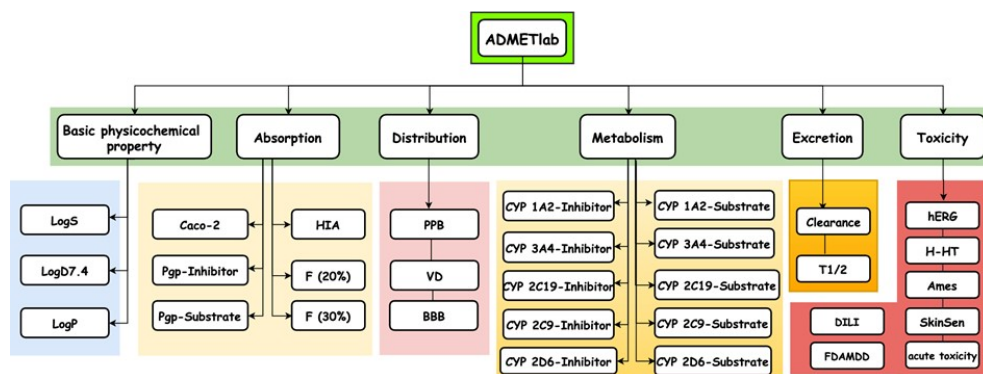**Fig. 7.** The detailed information about ADMET.

Fig. 8. A platform for systematic ADMET evaluation.

Table 2. PLS Statistics of CoMFA and CoMSIA models.

Model	Q²	R²	Save	F	N	R²ext	Fractions				
							Ster	Elec	Acc	Don	Hyd
CoMFA	0.614	0.970	0.098	163.736	3	0.778	0.417	0.583	-	-	-
CoMSIA	0.583	0.902	0.172	74.043	2	0.972	0.142	0.235	0.189	0.260	0.173

Q^2: Cross-validated determination coefficient. N: Optimum number of components. R^2: Non-cross- validated determination coefficient. S_{cv}: Standard error of the estimate. F: F-test value. R^2_{ext}: External validation determination coefficient

Table 3. Actual and predicted pIC50 along with residual training and test sets using CoMFA and CoMSIA models.

| Nº	pIC$_{50}$(observed)	CoMFA		CoMSIA	
		Predicted	Residuals	Predicted	Residuals
1*	8.1	8.207	-0.107	7.34	0.76
2	7.7	7.785	-0.085	6.92	0.78
3*	7.5	8.107	-0.607	7.59	-0.09
4	7.9	7.944	-0.044	7.18	0.72
5	7.2	7.204	-0.004	7.13	0.07
6	7.4	7.256	0.144	7.13	0.27
7	8.5	8.435	0.065	7.29	1.21
8	8.4	8.462	-0.062	7.28	1.12
9*	8.8	8.396	0.404	8.19	0.61
10*	8.6	8.535	0.065	8.48	0.12
11	8.7	8.603	0.097	7.02	1.68
12	8.5	8.427	0.073	7.05	1.45
13	8.5	8.564	-0.064	6.77	1.73
14	8.8	8.767	0.033	8.08	0.72
15	8.1	8.147	-0.047	7.99	0.157
16	8.8	8.764	0.036	7.99	0.81
17	8.7	8.645	0.055	8.21	0.49
18	8.8	8.760	0.04	8.19	0.61
19	8.7	8.748	-0.048	8.22	0.48
20	8.8	8.824	-0.024	8.67	0.13
21	9.1	9.008	0.092	8.85	0.25
22	8.7	8.702	-0.002	7.88	0.82
23	8.2	8.457	-0.257	8.64	-0.44

* Test set molecules.
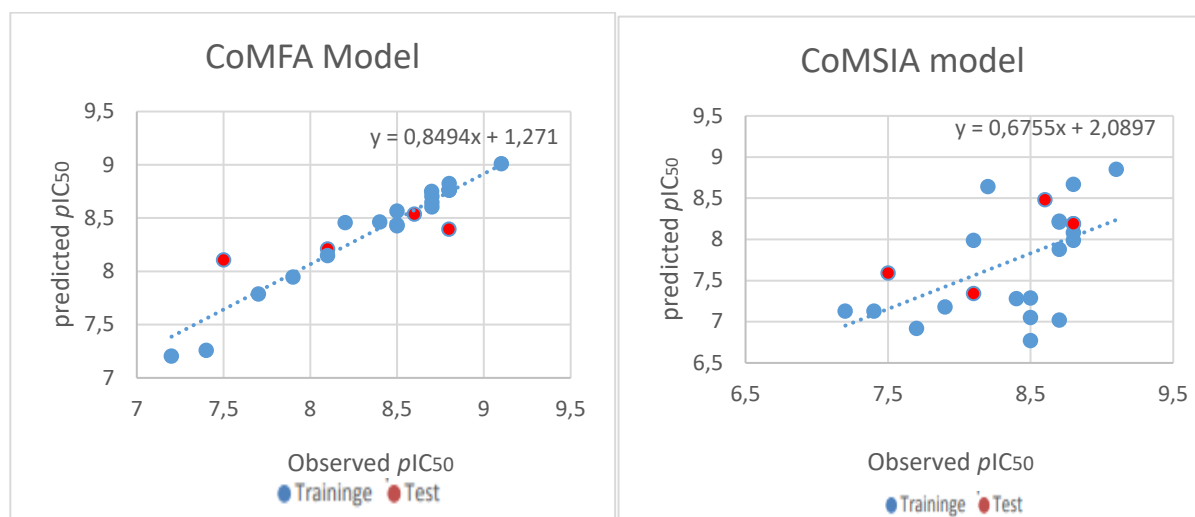
Fig. 9. Graphical representation of the observed and predicted activity of training and test sets for CoMFA and CoMSIA models.

Interpretation of CoMFA and CoMSIA results

In the 3D-QSAR study, the variation of the biological activity is combined with the variation of the organic fields and properties that cause the change of grouping on the molecules that bear the same basic structure in this technique found two methods which are known CoMFA and CoMSIA. These two methods are based on the same principle and make it possible to visualize the changes which take place in each field at the level of the contour maps in three-dimensional space for the components that bear the same skeleton, this last can lead to an increase or decrease of study activity. Figure 10 shows the steric (S) and electrostatic (E) contour maps of model CoMFA. Moreover, Figure 11 shows the contour maps of the CoMSIA model of the fields: steric (S), electrostatic (E), hydrophobic (H) acceptors, and donors of hydrogen bonds (HBA) & (HBD). All contours represented respectively the default contributions of 80% and 20% for the favored and disadvantaged regions.
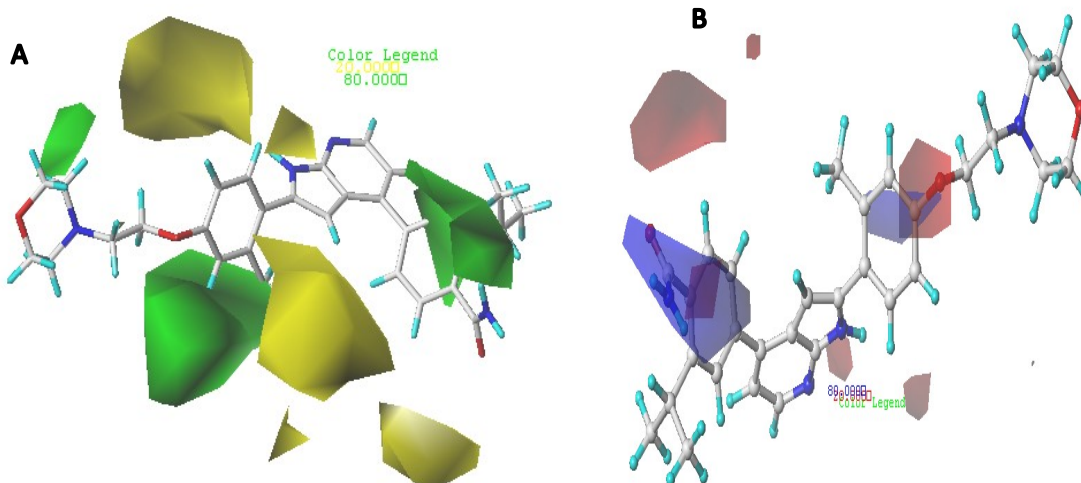
CoMFA contour maps analysis

We have carried out the CoMFA model on the most active compound 21 (pIC_{50} = 9.1) which was used as a reference structure. The presentation of the CoMFA model in Figure 10 visualizes the electrostatic contributions that are indicated by red and blue colors, and both the steric contributions which are shown by green and yellow outline colors. After this analysis, we notice that around the green regions the bulky substitutes are favored. Moreover, the yellow areas of the bulky groups are disadvantaged. We found that in the steric field there is a green outline that covers part of R 3 = CH_3 donor by inductive effect , which suggests that the effect of the inhibitor on these large groups at this position should be higher. Also, we observed that in the electrostatic field a blue zone is located near the position R1 = $CONH_2$ which is both attractors by mesomeric effect and inductive effect, indicates that the electropositive groups at this position reinforce the anti-obesity activity. Thus, a red contour map covers the part of R4 = 4-O (CH_2) 2-morpholine donor by indicative effect, shows that all the electronegative groups in this part would present a high inhibitory activity of CaMKKII.

Fig. 10. Contour maps of CoMFA analysis. **A)** Steric fields; **B)** Electrostatic fields.

CoMSIA contour maps analysis

According to the PLS statistical results associated with

the CoMSIA model, which are grouped together in Table 2, we observed that the fractions of the different fields are: S =

14.2%, E = 23.5%, H = 17.3%, HBD = 26% and HBA = 18.9%. Thus, in Figure 11A, we visualized that the contours of the CoMSIA steric field were located in a similar way to that of the CoMFA model (Figure 10A). Also, we have seen in Figure 11B that the blue region (80% contribution) around the R3 substituent indicates that the groups with electro-donor characters can develop the CaMKKII inhibitory activity, while the red (20% contribution) is around the R4 position could enhance the potency of this activity.

The hydrophobic substances are soluble in nonpolar solvents such as benzene but little or not soluble in water. Figure 11C is indicated the hydrophobic region ("hatred of water"), this yellow outline (80% contribution) is around the position R3 = CH3 shows that the substituents with a hydrophobic character because all the bonds around the carbon atom are occupied therefore the chemical group, is described as being nonpolar which can increase the activity. Whereas the white outline (20% contribution) which is close to the R4 position indicates that groups with a hydrophilic character are favored. In CoMSIA HBD outline maps (Figure 11D), the cyan (80% contribution) outlines around the R1 position and a certain position indicates that amine with the hydrogen bond donor trait may enhance activity. In Figure 11E, the outline of magenta (80% contribution) around the R4 position shows that groups with a hydrogen bond donor character in this position can derive potency. While the red (20% contribution) outline around the R3 position shows that only groups with hydrogen bond donors can enhance activity.
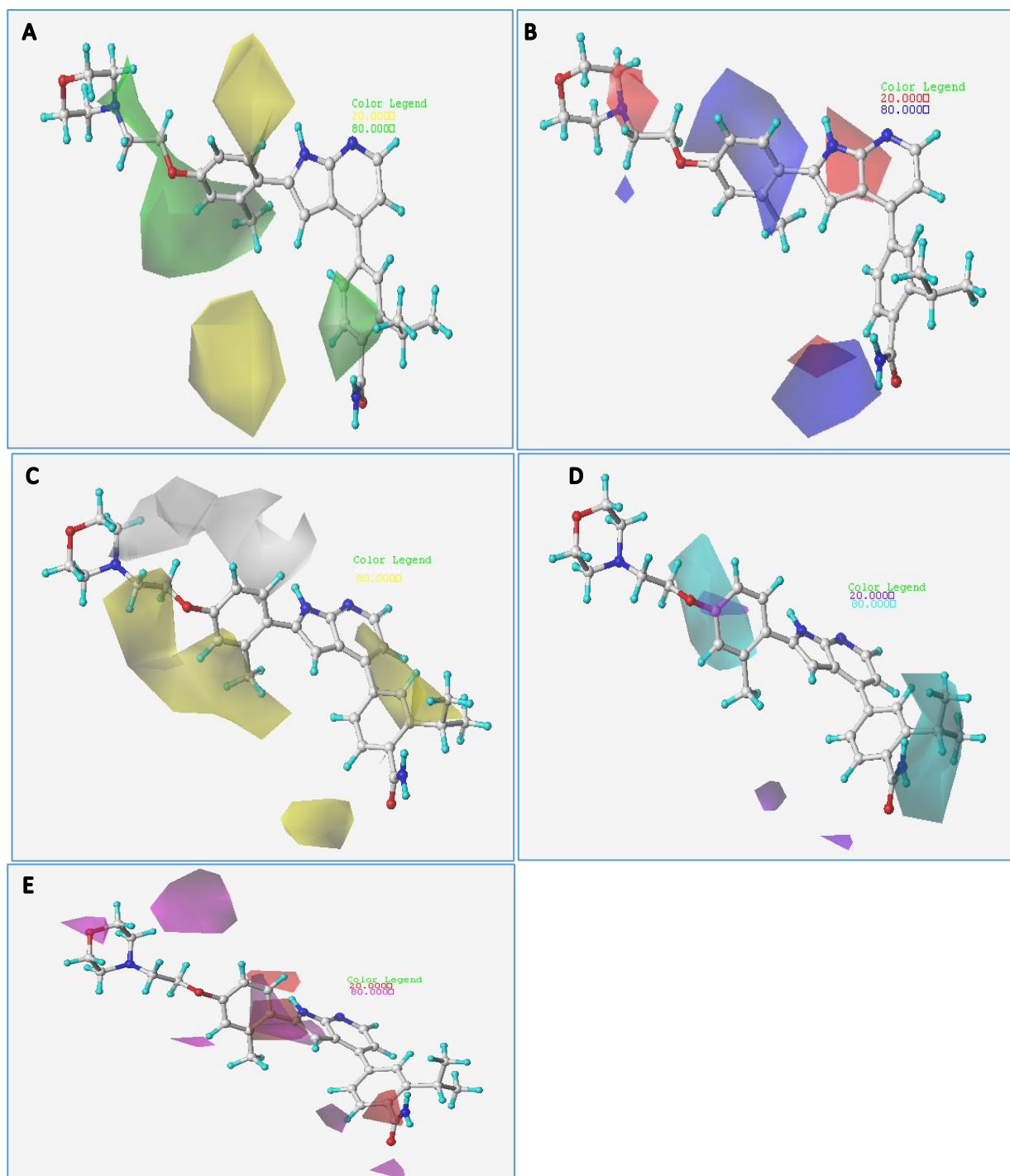

Fig. 11. Contour maps of CoMSIA analysis. **A)** Steric field; **B)** Electrostatic field; **C)** Hydrophobic field; **D)** H-bond acceptor field; **E)** H-bond donor field.

Quality check of the planned model

In this study we looked at various structural validation programs that are carried out to verify and evaluate the quality of protein models, they were designed using programs such as Procheck, ERRAT, and Prosaweb. The modeled protein pdb:2ZV2 was validated by the presence of the PROCHECK program which was used to perform Ramachandran plot calculations for geometry as well as the stereochemical quality of proteins. The latter indicates the stereochemistry of the Phi, Psi (φ, ψ) twisting angles of the main chain of a better protein model. The Ramachandran graph showed that 89.3% of the tailings were in the most favorable zone, 9.4% in the allowed region while only 0.4% in the outlier region (Figure 12C). Furthermore, we called the ProsaWeb program to perform the Z-score derived from the -6.45 model, which indicates that the model represents a nuclear magnetic resonance (NMR) quality structure (Figure 12B). Moreover, the overall quality value for this structure is 89.95%, it visualized from the ERRAT program (Figure 12D), which confirms that the predicted model is good enough to use it [38].

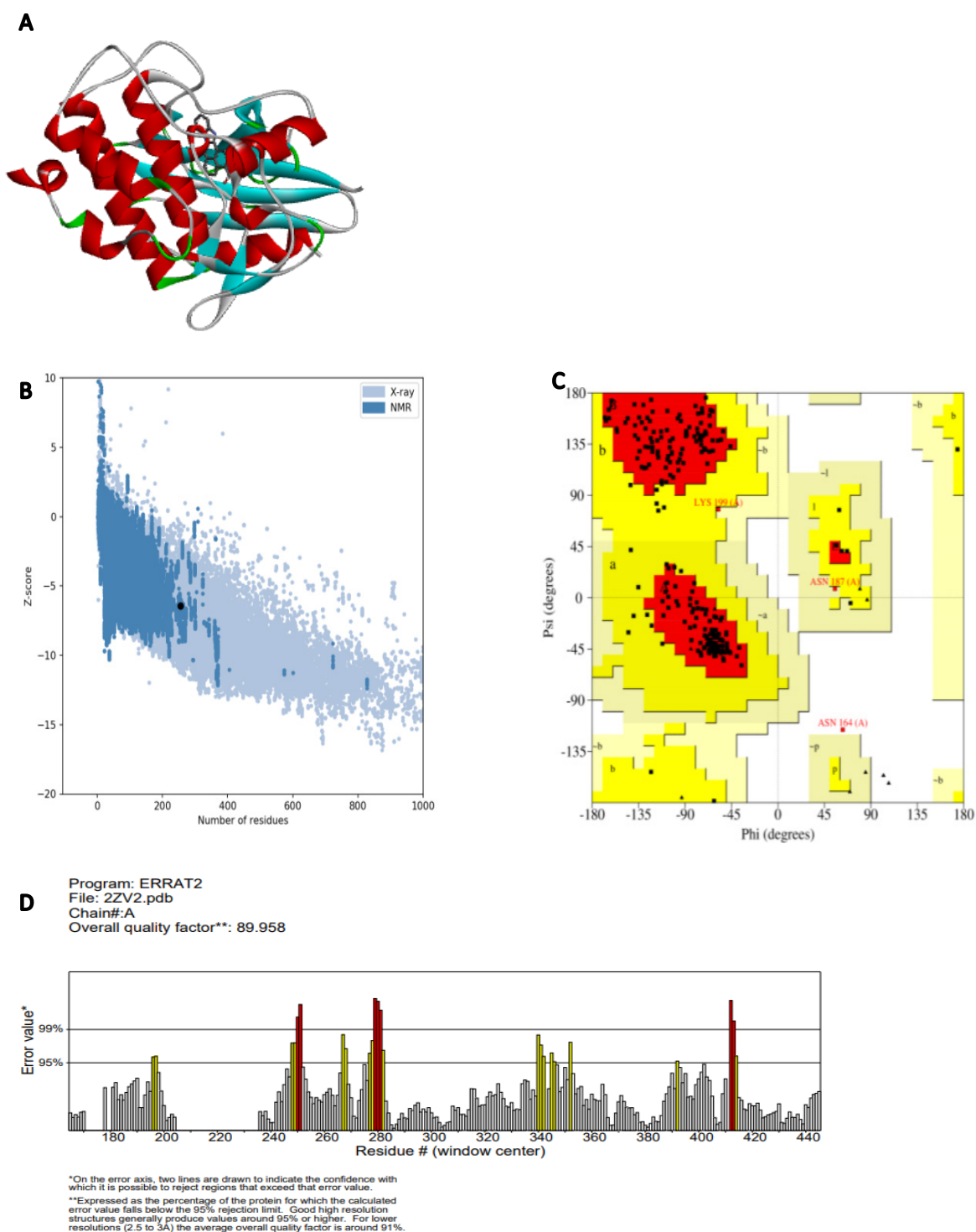**Fig. 12. A**) Three-dimensional representation of modeled 2ZV2; **B**) Z-Score plot for the modeled 2ZV2, and **C**) Ramachandran plot statistics for modeled 2ZV2. **D**) Illustration of ERRAT plot analysis for the overall quality factor of 2ZV2.

Docking results

To study the interaction of the two molecules, the more active 21 (*p*IC$_{50}$ = 9.1; E = 2.9613 Kcal/mol) and the inactive 5 (*p*IC$_{50}$ = 7.2; E = 4.4627 Kcal/mol) with the protein (PDB ID: 2ZV2; Resolution: 2.40 Å), we applied the surflex-docking method by using the SYBYL program. The 3D binding mode of these compounds is illustrated in Figure 13. A molecular docking study of the most active compound (21) was performed to clarify the probable binding modes between pyrimidine and azaindole derivatives with our target (2ZV2), which provides simple knowledge for additional structural

optimization. The most powerful compound 21 showed Pi-sigma interaction with SER 317 and ALA 330, as well as carbon hydrogenic bond interactions and Pi-Donor Hydrogen Bond forms residues PHE 268; TYR177 and GLU 278, plus the presence of Pi-Anion with ASP 331 and the existence of Pi-Alkyl interaction between the VAL 180, LEU 320 and PRO 275 groups, while the hydrogen bonding interaction with LYS 174 explains their high activity. While our protein forms with the inactive molecule an unfavorable donor-donor interaction GLY 274, which explains its lower activity, according to the results we also found that the lowest docking score indicating the binding affinity higher.
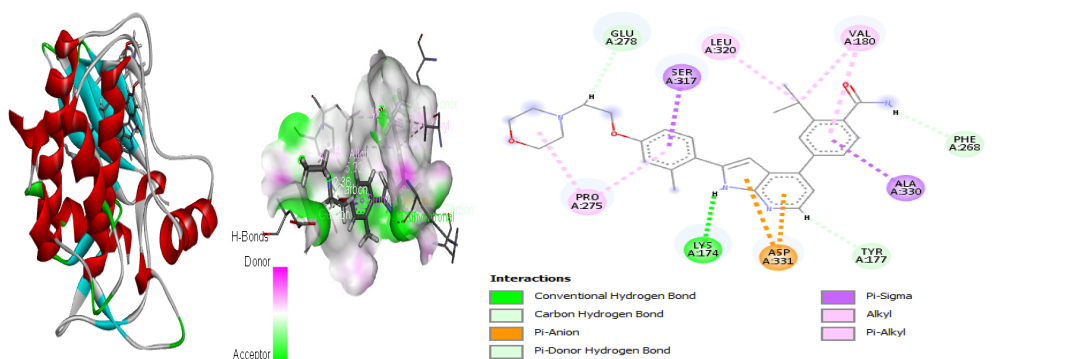

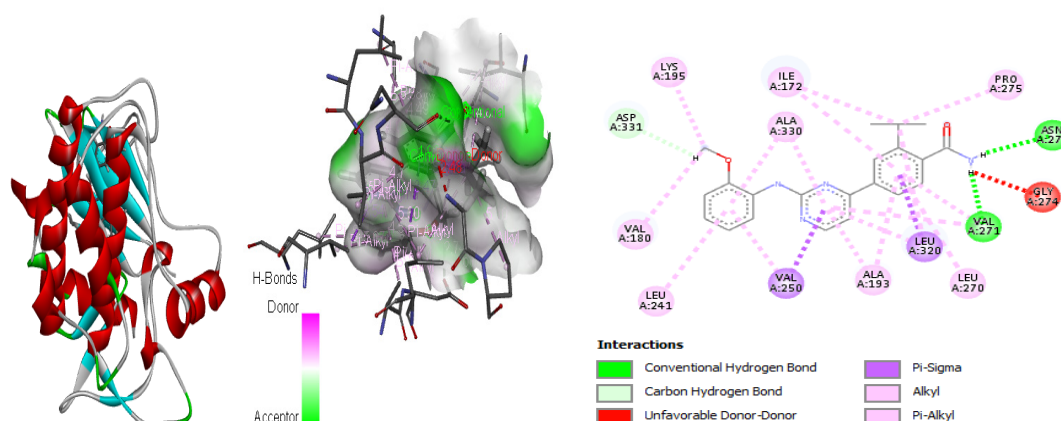**Fig. 13.** Interactions of active compound in the site of CAMKKII receptor (PDB code: 2ZV2).

Fig.14. Interactions of the inactive compound in the site of CAMKKII receptor (PDB code: 2ZV2).

ADMET

In this part, we will focus on the least active (5) and the most active (21) molecules which have a percentage of crossing the blood-brain barrier (BBB) 0.144% and 1.104% respectively which indicates that these molecules weakly cross this barrier. These two molecules exhibit low solubility. Furthermore, these molecules have a percentage of binding with plasma proteins of 85.403% and 83.350% and have a percentage of absorption in the intestinal lumen of 94.598% and 94.079%. About the reaction of these molecules towards.

In view of certain CYPs, these molecules have a high chance of not being inhibitors for CYP_2C19 and a low chance of being substrates for CYP_3A4. Also, these molecules are not P-glycoprotein inhibitors.

These molecules pose a medium-risk of cardiac toxicity through potassium channel inhibition (hERG). Thus, we must test these molecules experimentally for this toxicity to ensure these results the parameters obtained from the calculations of the ADMET analysis are given in Tables 4 and 5.

Table 4. In silico ADME for the most active 21 molecules and the least active 5.

N	BBB	BS	Inhibition				Substrate		HIA%	Pgp. I	PPB
			CYP_2C19_	CYP_2C9_	CYP_2D6_	CYP_3A4	CYP_2D6_	CYP_3A4_			
5	0.144	1.99	Non	Non	Non	Non	Non	Weakly	94.598	Non	85.403
21	1.101	0.084	Non	Yes	Non	Yes	Non	Yes	94.079	Non	83.350

BBB = blood-brain barrier penetration. **BS** = Buffer Solubility (mg/l). **CYP2C19** = cytochrome p4502C19, **CYP2C9** = cytochrome p4502C9, **CYP3A4** = cytochrome p4503A4, **CYP2D6** = cytochrome CYP2D6, **PgP I** = P-glycoprotein inhibition, **PPB** = plasma Protein Binding %, **HIA** = human intestinal absorption %.

Table 5. Toxicity molecules 5 and 21.

ID	Carcino_Rat	hERG_inhibition	TA100_10RLI	TA100_NA	TA1535_10RLI	TA1535_NA
5	negative	medium_risk	negative	negative	positive	negative
21	negative	medium_risk	positive	negative	negative	negative

4. Conclusions

Based on the research that has been carried out, a series of 23 molecules built on pyrimidine and azaindole derivatives were used to study the CAMKKII inhibitory activity against obesity with varying values of pIC$_{50}$ activity (7.2–9.1), by using different computer-aided drugs techniques. The 3D-QSAR and molecular docking studies were used to predict the CAMKKII inhibitory activity of this set of molecules, which is established to give satisfactory statistical results. The CoMFA and CoMSIA models established in this study have been validated internally and externally to explore the structure-activity relationship. The current study showed excellent internal and external results for CoMFA (Q^2 = 0.614, R^2 = 0.970, R^2_{ext} = 0.778) and CoMSIA (Q^2 = 0.583, R^2 = 0.902, R^2_{ext} = 0.972). Based on the graphical interpretation of the optimal results derived from the CoMFA and CoMSIA contour maps, several structural features in terms of favorable and unfavorable substitutions were revealed which could enhance the inhibitory activity of CAMKKII. Thus, the docking results provided quantitative binding affinities of ligands to the active site of CaMKKII receptor and revealed the critical role of Val 180, ILE 172, PHE 268 and TYR 177 in binding of inhibitors to the active site. Moreover, the results of ADMET is of great help for discovering new drugs against obesity, and avoiding to fall on severe cases if we have been infected with Covid-19.

Acknowledgments

Author Contributions

All authors confirmed they have contributed to the intellectual content of this paper and have met the following requirements: significant contributions to the conception and design, acquisition of data, or analysis and interpretation of data; drafting or revising the article for intellectual content; and final approval of the published article. **Participation of authors by task:** Hajji Halima, Fatima En-nahli and Ilham Aanouz concept, design and perform the study;Hajji Halima, Fatima En-nahli, Mohammed Aziz Ajana and Mohammed Bouachrine develop the methodology;Hajji Halima, Fatima En-nahli, Ilham Aanouz and Mohammed Aziz Ajana write the original draft; Hajji Halima, Fatima En-nahli and Mohammed Aziz Ajana validate the data obtained; Hajji Halima, Hanane Zaki,Tahar Lakhlifi and Mohammed Bouachrine analyse and validate the data; all authors revise, edit and approve the submitted article; Mohammed Aziz Ajana and Mohammed Bouachrine supervise the study.

.

References and Notes

[1] Zhou, Y.; Chi, J.; Lv, W.; Wang, Y. *Diabetes Metab. Res. Rev*. **2020**, *37*, e3377. [Crossref]

[2] Scheen, A. J. *Med. des Mal. Metab*. **2020**, *14*, 437. [Crossref]

[3] Finelli, C. *Immunotherapy*. **2020**, *12*, 1105. [Crossref]

[4] Belančić, A.; Kresović, A.; Rački, V. *Obes. Med*. **2020**, *19*, 100259. [Crossref]

[5] Palaiodimos, L.; Kokkinidis, D. G.; Li, W., Karamanis, D.; Ognibene, J.; Arora, S.; Southern, W. N.; Mantzoros, C. S.; *Metab. Clin. Exp*. **2020**, *108*, 154262. [Crossref]

[6] Dixon, A. E.; Peters, U. *Expert Rev. Respir. Med*. **2018,** *12*, 755. [Crossref]

[7] Caussy, C.; Wallet, F.; Laville, M.; Disse, E. *Obesity*. **2020**, *28*, 1175. [Crossref]

[8] Richardson, S.; Hirsch, J. S.; Narasimhan, M.; Crawford, J. M.; McGinn, T.; Davidson, K. W. et al. *JAMA Netw*. **2020**, *323*, 2052. [Crossref]

[9] Vardell, E. *Med. Ref. Serv. Q*. **2020**, *39*, 67. [Crossref]

[10] Gao, F.; Zheng, K. I.; Wang, X.-B.; Sun, Q.-F.; Pan, K.-H.; Wang, T.-Y.; Chen, Y.-P.; Targher, G.; Byrne, C. D.; George, J.; Zhen, M.-H. *Diabetes Care* **2020**, *43*, e72. [Crossref]

[11] Morgan, O. W.; Bramley, A.; Fowlkes, A.; Freedman, D. S.; Taylor, T. H.; Gargiullo, P.; Belay, B.; Jain, S.; Cox, C.; Kamimoto, L.; Fiore, A.; Finelli, L.; Olsen, S. J.; Fry, A. M. *PLoS One*. **2010**, *5*, e9694. [Crossref]

[12] Díaz, E.; Rodríguez, A.; Martin-Loeches, I.; Lorente, L.; del Mar Martín, M.; Pozo, J. C; Carlos, M. J.; Angel, E.; Ángel, A.; Jordi, R. et al. *Chest*. **2011**, *139*, 382. [Crossref]

[13] Lighter, J.; Phillips, M.; Hochman, S.; Sterling, S.; Johnson, D.; Francois, F.; Stachel, A. *Arch. Clin. Infect. Dis*. **2020**, *71*, 896. [Crossref]

[14] Cai, Q.; Chen, F.; Wang, T.; Luo, F.; Liu, X.; Wu, Q.; He, Q.; Wang, Z.; Liu, Y.; Liu, L.; Chen, J.; Xu, L. *Diabetes Care* **2020**, *43*, 1392. [Crossref]

[15] Anderson, K. A.; Ribar, T. J.; Lin, F.; Noeldner, P. K.; Green, M. F.; Muehlbauer, M. J.; Witters, L. A.; Kemp, B. E.; Means, A. R. *Cell Metab*. **2008**, *7*, 377. [Crossref]

[16] Hajji, H.; Aanouz, I.; Khatabi, K. E.; Lakhlifi, T.; Ajana, M. A.; Bouachrine, M. *JASAB*. **2020**, *2*, 23. [Crossref]

[17] Profeta, G. S.; dos Reis, C. V.; Santiago, A. S.; Godoi, P. H. C.; Fala, A. M.; Wells, C. I.; Sartori, R.; Salmazo, A. P. T.; Ramos, P. Z.; Massirer, K. B.; Elkins, J. M.; Drewry, D. H.; Gileadi, O.; Couñago, R. M. *Sci. Rep*. **2019**, *9*, 16452. [Crossref]

[18] Marcelo, K. L.; Ribar, T.; Means, C. R.; Tsimelzon, A.; Stevens, R. D.; Ilkayeva, O.; Bain, J. R.; Hilsenbeck, S. g.; Newgard, C. B.; Means, A. R.; York, B. *J. Mol. Endocrinol*. **2016**, *30*, 557. [Crossref]

[19] Heini, A.; Lara-Castro, C.; Kirk, K.; Considine, R.; Caro, J.; Weinsier, R. *Int. J. Obes*. **1998**, *22*, 1084. [Crossref]

[20] O'Byrne, S. N.; Scott, J. W.; Pilotte, J. R.; Santiago, A. S.; Langendorf, C. G.; Oakhill, J. S.; Eduful, B. J.; Couñago, R. M.; Wells, C. I.; Zuercher, W. J.; Wilson, T. M.; Drewry, D. H. *Molecules*. **2020**, *25*, 325. [Crossref]

[21] Klok, M. D.; Jakobsdottir, S.; Drent, M. L. *Obes. Rev*. **2007**, *8*, 21. **[Crossref]**

[22] Aouidate, A.; Ghaleb, A.; Ghamali, M.; Chtita, S.; Ousaa, A.; Choukrad, M.; Sbai, A.; Bouachrine, M.; Lakhlifi, T. *Chem. Zvesti*. **2018**, *72*, 2833. **[Crossref]**

[23] Kubinyi, H. *The Encyclopedia of Computational Chemistry* **1998**, *1*, 448. **[Crossref]**

[24] Klebe, G.; Abraham, U.; Mietzner, T. *J. Med. Chem*. **1994**, *37*, 4130. **[Crossref]**

[25] Price, D. J.; Drewry, D. H.; Schaller, L. T. et al. *Bioorganic Med. Chem. Lett*. **2018**, *28*, 1958. **[Crossref]**

[26] M.O. St. Louis, SYBYL-X, version 2.0. Tripos Associates, USA, 2012.

[27] Clark, M; Cramer, R. D.; Van Opdenbosch, N. *J. Comput. Chem*. **1989**, *10*, 982. **[Crossref]**

[28] Purcell, W. P.; Singer, J. A. *J. Chem. Eng. Data*. **1967**, *12*, 235. **[Crossref]**

[29] AbdulHameed, M. D. M.; Hamza, A.; Liu, J.; Zhan, C.-G. *J. Chem. Inf. Model*. **2008**, *48*, 1760. **[Crossref]**

[30] Ståhle, L.; Wold, S. *Prog. Med. Chem*. **1988**, *25,* 291. **[Crossref]**

[31] Bush, B. L.; Nachbar, R. B. *J. Comput. Aided Mol. Des*. **1993**, *7*, 587. **[Crossref]**

[32] El Khatabi̇, K.; Aanouz, İ.; El-Merni̇Ssi̇, R.; Khaldan, A.; Ajana, M. A.; Bouachrine, M.; Lakhlifi, T. *J. Turkish Chem. Soc. Sect. Chem*. **2020**, 469. **[Crossref]**

[33] Kuntz, I. D.; Blaney, J. M.; Oatley, S. J.; Langridge, R.; Ferrin, T. E. *J. Mol. Biol*. **1982**, *161*, 269. **[Crossref]**

[34] Kitchen, D. B.; Decornez, H.; Furr, J. R.; Bajorath, J. *Nat. Rev. Drug Discov*. **2004**, *3*, 935. **[Crossref]**

[35] Barril, X.; Soliva, R. *Mol. Biosyst*. **2006**, *2*, 660. **[Crossref]**

[36] Ningombam, S.; Kumar, R.; Tanwar, P. *Wiener Klinische Wochenschrift*. **2021**, *133*, 383. **[Crossref]**

[37] Ramos, J. Modelización y Simulación en Ciencias de la Vida usando Discovery Studio. 2020.

[38] Hajji, H.; En-Nahli, F.; Abdessadak, O.; El Khatabi, K.; Ajana, M. A.; Lakhlifi, T.; Bouachrine, M. *RHAZES: Green Appl. Chem*. **2021**, *12*, 40. **[Crossref]**

How to cite this article